Journal of Sound and Vibration (1999) **219**(1), 157–174
Article No. jsvi.1998.1906, available online at http://www.idealibrary.com.on IDEAL

FURTHER RESULTS FOR MODAL CHARACTERISTICS OF ROTATING TAPERED TIMOSHENKO BEAMS

A. BAZOUNE, Y. A. KHULIEF

Department of Mechanical Engineering, King Fahd University of Petroleum and Minerals, KFUPM Box 579, Dhahran 31261, Saudi Arabia

AND

N. G. STEPHEN

Department of Mechanical Engineering, The University, Southampton, SO17 1BJ, U.K.

(*Received* 29 *January* 1998, *and in final form* 12 *August* 1998)

The in-plane and out-of-plane modes of free vibration of a tapered Timoshenko beam mounted on the periphery of a rotating rigid hub are investigated. The finite element method is used to discretize the beam. This formulation permits unequal breadth and depth taper ratios as well as unequal element lengths. The effects of shear deformation, rotary inertia, hub radius, setting angle, and spinning rotation are considered. The generalized eigenvalue problem is defined using explicit expressions for the mass and stiffness matrices and numerical solutions are generated for a wide range of parameter variations. Explicit expressions of Southwell coefficients are presented for the first time for the case of rotating uniform and tapered Timoshenko beams. Comparisons are made wherever possible with exact solutions and other numerical results available in the literature. Extended results are obtained to serve as a benchmark solution for other numerical techniques and specialized applications.

1. INTRODUCTION

The dynamic characteristics (natural frequencies and associated mode shapes) of rotating tapered beams is of great importance to the design and performance evaluation in a variety of engineering applications, including helicopter blading, robot manipulators and spinning space structures, and has been the subject of interest to many investigators.

Compared to rotating uniform and tapered Euler–Bernoulli beams [1–11], the problem of rotating tapered Timoshenko beams has received less attention inspite of its importance to many engineering systems. Moreover, solutions reported in the current literature are less than adequate when compared to the simpler case of the rotating uniform Euler–Bernoulli beams. Because of the complexity of the

0022–460X/99/010157 + 18 $30.00/0

problem, an exact solution is impossible and many approximate mathematical models have been developed to investigate the dynamic behavior of such rotating beams. Some studies have tackled the problem of rotating uniform Timoshenko beams [12–15]. Recently, Bazoune and Khulief [16] developed a finite beam element for vibration analysis of a rotating doubly tapered Timoshenko beam in which explicit expressions for the finite element mass and stiffness matrices were derived using the consistent mass approach. Later, Khulief and Bazoune [17] extended the work in reference [16] to account for different combinations of the fixed, hinged and free end conditions. The simulation results presented in references [16] and [17] are only for the out-of-plane vibration of rotating tapered Timoshenko beams where the effect of hub radius and setting angle were not considered. Mulmule *et al.* [18] presented a formulation similar to the one presented in reference [14] but for a tapered beam. However, no explicit expressions for the element matrices were given in reference [18]. In addition to the comment made by Naguleswaran [19] on the results reported in reference [18], few simulation results were presented graphically for the case of a rotating tapered Timoshenko beam. Hsieh and Abel [20] presented a very general formulation for rotating bladed disk assemblies where no specific expressions of the elemental matrices were given. Only the first two frequencies of rotating tapered Timoshenko beam were presented.

The survey of the current literature reveals a shortage of solution results pertinent to rotating tapered Timoshenko beams. In this paper, the work of reference [16] is extended to include the effect of hub radius and in-plane vibration. Explicit expressions of Southwell coefficients are presented for the first time for the case of rotating uniform and tapered Timoshenko beams. Extended results are presented here for the first time to serve as a benchmark solution for other numerical techniques and specialized applications. The solutions obtained include numerous combinations over a wide range of parameter variations.

2. THE FINITE ELEMENT MODEL

Figure 1 shows a typical rotating tapered cantilever beam model in the deformed state. In this figure, the (XYZ) axes represent a global orthogonal co-ordinate system with origin at the center of mass of the hub such that the Z-axis corresponds to the spin axis which rotates with a constant angular speed Ω. The $(X'Y'Z')$ system is defined as a system of local co-ordinates parallel to the global (XYZ) co-ordinate system and rigidly attached to the root of the beam with its origin shifted by R_0 from the global (XYZ) co-ordinate system. The co-ordinate system (xyz) represents a body co-ordinate system that is rigidly attached to the root of the beam and is obtained by rotating the $(X'Y'Z')$ co-ordinate system about the X'-axis by an angle ψ called the setting angle. The X, X' and x-axes being collinear and coincident with the undeformed beam centerline while the y- and z-axes lie along the principal axes of the cross-sectional area of the beam. The beam undergoes flexural vibration in a plane fixed in a local system and rotating with the beam. For $\psi = 90°$, the vibration is in the plane of rotation and for $\psi = 0°$, the vibration is out of the plane of rotation. It is assumed that: (1) the

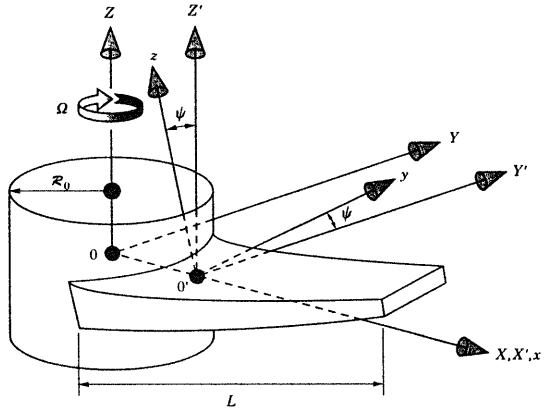

Figure 1. The rotating tapered beam configuration at deformed state.

material of the beam is elastic, homogeneous and isotropic, (2) the linear theory of elasticity is applied, (3) the hub is rigid, (4) the plane cross-sections initially perpendicular to the neutral axis of the beam remain plane but no longer perpendicular to the neutral axis after deformation, and (5) the shear center of the beam cross-section coincides with its centroid, the cross-section being doubly symmetric.

The finite element method is used to discretize the elastic beam. The beam configuration can be defined by a properly generated mesh of finite beam elements. In this formulation, beam elements are linearly tapered in two planes. Any combination of taper ratios in the two planes is permitted.

2.1. THE DISPLACEMENT FIELD

According to Timoshenko beam theory, the total deflection $w^i(x^i, t)$ of the ith beam element at a point x^i consists of two parts, one caused by bending deformation $w_b^i(x^i, t)$ and one by shear deformation $w_s^i(x^i, t)$, so the total deflection can be expressed as

$$w^i(x^i, t) = w_b^i(x^i, t) + w_s^i(x^i, t), \tag{1}$$

The slope of the deflection curve at point x^i can be written as

$$\frac{\partial w^i(x^i, t)}{\partial x^i} = \frac{\partial w_b^i(x^i, t)}{\partial x^i} + \frac{\partial w_s^i(x^i, t)}{\partial x^i}$$

$$= \theta^i(x^i, t) + \gamma^i(x^i, t), \tag{2}$$

where the angles θ^i and γ^i are due to bending deformation and shear deformation, respectively. Taking the effect of shear deformation into account, the transverse

displacement w^i, and the bending rotation θ^i at an arbitrary point p^i on element (i) with respect to the element axes can be expressed as

$$w^i(x^i, t) = [\mathbf{N}_w^i(x^i)]\{\mathbf{q}^i(t)\} \quad \text{and} \quad \theta^i(x^i, t) = [\mathbf{N}_\theta^i(x^i)]\{\mathbf{q}^i(t)\}, \tag{3}$$

where $w^i(x^i, t)$ and $\theta^i(x^i, t)$ represent the elastic deformations of the beam element, $[\mathbf{N}_w^i(w^i)]$ and $[\mathbf{N}_\theta^i(x^i)]$ are the matrices of shape functions that are used to model the deformations of the beam element. In this formulation, a two-node element is adopted. If the nodal variables are the transverse displacement w^i, and the bending rotation θ^i, then the nodal co-ordinate vector $\{\mathbf{q}^i\}$ defined as

$$\{\mathbf{q}^i(t)\} = [w_1^i, \theta_1^i, w_2^i, \theta_2^i]^T. \tag{4}$$

Equation (3) is a general equation and is valid for any type of shape functions $[N^i]$ used to model the beam element. However, the shape functions adopted in this work are the usual Hermitian polynomials and incorporate in addition to the continuity and completeness conditions a shear deformation parameter that accounts for Timoshenko beams. The explicit expressions of the entries of the matrices $[N_w^i]$ and $[N_\theta^i]$ are given in reference [14].

2.2. STRAIN ENERGY EXPRESSION

Following the notation of reference [16], the strain energy expression of the *ith* non-spinning tapered Timoshenko beam element of length l^i is given by

$$U_e^i = \tfrac{1}{2}\{\mathbf{q}^i\}^T[\mathbf{K}_e^i]\{\mathbf{q}^i\} + \tfrac{1}{2}\{\mathbf{q}^i\}^T[\mathbf{K}_s^i]\{\mathbf{q}^i\}, \tag{5}$$

where $[\mathbf{K}_e^i]$, and $[\mathbf{K}_s^i]$ are the elemental bending stiffness matrix, and the elemental shear stiffness matrix, respectively. The explicit expressions of the entries of these respective elemental matrices $[\mathbf{K}_e^i]$, and $[\mathbf{K}_s^i]$ are given in reference [16].

The strain energy expression for the ith spinning tapered Timoshenko beam element of length l^i due to axial stresses resulting from the centrifugal force field can be given by

$$U_c^i = \tfrac{1}{2}\{\mathbf{q}^i\}^T[\overline{\mathbf{K}_c^i}]\{\mathbf{q}^i\}, \tag{6}$$

where $[\overline{\mathbf{K}_c^i}]$ is the elemental centrifugal stiffness matrix given by

$$[\overline{\mathbf{K}_c^i}] = \int_0^{l^i} [\mathbf{B}_c^i]^T \overline{F_p^i}(x^i)[\mathbf{B}_c^i]\, \mathrm{d}x^i, \tag{7}$$

where

$$[\mathbf{B}_c^i] = \frac{\partial}{\partial x^i}[\mathbf{N}_w^i] \tag{8}$$

and $\overline{F_p^i}(x^i)$ is the centrifugal force acting on the beam as a consequence of the spinning rotation of the hub. Here the assumption has been made that the displacements are sufficiently small such that the higher order terms of the change in the axial direction (x-axis) of an element can be neglected. The expression of

the tensile force $\overline{F_p^i}(x^i)$ acting on a section of the beam and associated with a differential element at point p^i of the ith finite beam element is

$$\mathrm{d}\overline{F_p^i}(x^i) = \rho^i A^i(x^i)\Omega^2(R_0 + r_p^i)\, \mathrm{d}r_p^i, \tag{9}$$

where for small deformations, one can write

$$r_p^i = (L^i + x^i) = ((i-1)l^i + x^i). \tag{10}$$

The tensile force acting on a section at point p^i due to the centrifugal effect, can be calculated by integrating equation (9) over the span between point p^i and the free end of the beam as shown in Figure 2. The resulting tensile force is then determined, and may be expressed as

$$\overline{F_p^i}(x^i) = \frac{\rho^i A_0 \Omega^2}{L_{0y} L_{0z}}[-\beta_4 x^{i4} - \beta_3 x^{i3} - \beta_2 x^{i2} - \beta_1 x^i + \beta_0] = \Omega^2 F_p^i(x^i), \tag{11}$$

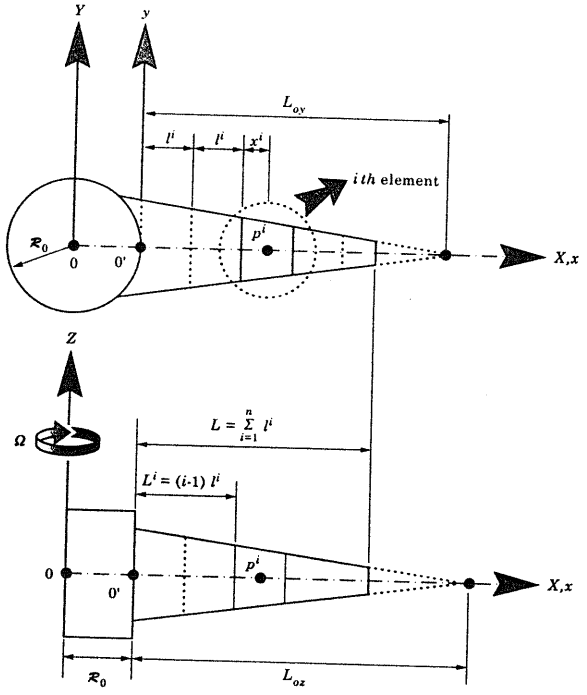

Figure 2. A beam element linearly tapered in two planes.

where

$$\beta_0 = \tfrac{1}{4}(n^4 - i^4 + \tfrac{4}{3}i - \tfrac{1}{3})l'^4 + \tfrac{1}{3}(-(2n^3 - 2i^3 + 3i - 1)\mu_2 + R_0(n^3 - i^3 + 1))l'^3$$
$$+ (\tfrac{1}{2}(n^2 - i^2 + 2i - 1)\mu_1 - R_0(n^2 - i^2 + 1)\mu_2)l'^2 + R_0(n - i + 1)\mu_1 l', \quad (12)$$

$$\beta_1 = \mu_1(R_0 + L'), \qquad \beta_2 = \tfrac{1}{2}(\mu_1 - 2\mu_2(R_0 + L')), \quad (13, 14)$$

$$\beta_3 = \tfrac{1}{3}((R_0 + L') - 2\mu_2), \qquad \beta_4 = \tfrac{1}{4}, \quad (15, 16)$$

where R_0 is the hub radius and L' is the inboard length of the beam element under consideration. If the hub radius R_0 is neglected, the expressions of $F_\rho^i(x^i)$ and β_i are rendered identical to those obtained in reference [16]. Now, equation (7) can be written as

$$[\overline{\mathbf{K}_c^i}] = \Omega^2[\mathbf{K}_c^i], \quad (17)$$

where

$$[\mathbf{K}_c^i] = \int_0^{l'} [\mathbf{B}_c^i]^T F_\rho^i(x^i)[\mathbf{B}_c^i]\,\mathrm{d}x^i. \quad (18)$$

TABLE 1

Centrifugal stiffness matrix of tapered Timoshenko beam element

$$[\mathbf{K}_c^i] = \frac{\rho^i A_0}{(1+\Phi)^2 L_{0i} L_{0z}}[\mathbf{K}_{ab}^{(c)}], \quad ab = 1, \ldots, 4$$

The non-zero entries of the lower triangular part of $[\mathbf{K}_{ab}^{(c)}]$ are as follows:

$$K_{11}^{(c)} = -K_{31}^{(c)} = K_{33}^{(c)} = \tfrac{1}{5}(5\Phi^2 + 10\Phi + 6)\beta_0 l'^{-1} - \tfrac{1}{10}(5\Phi^2 + 10\Phi + 6)\beta_1$$
$$- \tfrac{1}{105}(35\Phi^2 + 63\Phi + 36)\beta_2 l' - \tfrac{1}{140}(35\Phi^2 + 56\Phi + 30)\beta_3 l'^2$$
$$- \tfrac{1}{35}(7\Phi^2 + 10\Phi + 5)\beta_4 l'^3,$$

$$K_{21}^{(c)} = -K_{32}^{(c)} = -\tfrac{1}{10}\beta_0 + \tfrac{1}{60}(5\Phi^2 + 8\Phi + 6)\beta_1 l' + \tfrac{1}{420}(35\Phi^2 + 49\Phi + 30)\beta_2 l'^2$$
$$+ \tfrac{1}{280}(21\Phi^2 + 26\Phi + 14)\beta_3 l'^3 + \tfrac{1}{420}(28\Phi^2 + 31\Phi + 15)\beta_4 l'^4,$$

$$K_{22}^{(c)} = \tfrac{1}{60}(5\Phi^2 + 10\Phi + 8)\beta_0 l' - \tfrac{1}{120}(5\Phi^2 + 6\Phi + 4)\beta_1 l'^2 - \tfrac{1}{210}(7\Phi^2 + 7\Phi + 4)\beta_2 l'^3$$
$$- \tfrac{1}{1680}(49\Phi^2 + 44\Phi + 22)\beta_3 l'^4 - \tfrac{1}{420}(11\Phi^2 + 9\Phi + 4)\beta_4 l'^5,$$

$$K_{41}^{(c)} = -K_{43}^{(c)} = -\tfrac{1}{10}\beta_0 - \tfrac{1}{60}(5\Phi^2 + 8\Phi)\beta_1 l' - \tfrac{1}{420}(35\Phi^2 + 63\Phi + 12)\beta_2 l'^2$$
$$- \tfrac{1}{280}(21\Phi^2 + 40\Phi + 10)\beta_3 l'^3 - \tfrac{1}{420}(28\Phi^2 + 55\Phi + 15)\beta_4 l'^4,$$

$$K_{42}^{(c)} = -\tfrac{1}{60}(5\Phi^2 + 10\Phi + 2)\beta_0 l' + \tfrac{1}{120}(5\Phi^2 + 10\Phi + 2)\beta_1 l'^2 + \tfrac{1}{210}(7\Phi^2 + 14\Phi + 3)\beta_2 l'^3$$
$$+ \tfrac{1}{1680}(49\Phi^2 + 98\Phi + 22)\beta_3 l'^4 + \tfrac{1}{420}(11\Phi^2 + 22\Phi + 5)\beta_4 l'^5,$$

$$K_{44}^{(c)} = \tfrac{1}{60}(5\Phi^2 + 10\Phi + 8)\beta_0 l' - \tfrac{1}{120}(5\Phi^2 + 14\Phi + 12)\beta_1 l'^2 - \tfrac{1}{210}(7\Phi^2 + 21\Phi + 18)\beta_2 l'^3$$
$$- \tfrac{1}{1680}(49\Phi^2 + 152\Phi + 130)\beta_3 l'^4 - \tfrac{1}{420}(11\Phi^2 + 35\Phi + 30)\beta_4 l'^5,$$

Incorporating expression (11) into the integral of equation (7) and carrying out the integration of equation (7), the explicit expression of the centrifugal stiffness matrix $[\mathbf{K}_c^i]$ for the ith spinning tapered Timoshenko beam element of length l' due to centrifugal forces are given in Table 1.

The composite elemental stiffness matrix of the *ith* beam element can be written as

$$[\mathbf{K}^i] = [\mathbf{K}_e^i] + [\mathbf{K}_s^i] + \Omega^2[\mathbf{K}_c^i] \quad (19)$$

or

$$[\mathbf{K}^i] = [\mathbf{K}_{e,s}^i] + \Omega^2[\mathbf{K}_c^i], \quad (20)$$

where

$$[\mathbf{K}_{e,s}^i] = [\mathbf{K}_e^i] + [\mathbf{K}_s^i]. \quad (21)$$

2.3. KINETIC ENERGY EXPRESSION

The kinetic energy contribution due to translational and rotational deformation of the ith element of length l' is given by

$$T^i = \tfrac{1}{2}\{\dot{\mathbf{q}}^i\}^T[\mathbf{M}_t^i]\{\dot{\mathbf{q}}^i\} + \tfrac{1}{2}\{\dot{\mathbf{q}}^i\}^T[\mathbf{M}_r^i]\{\dot{\mathbf{q}}^i\}, \quad (22)$$

where

$$[\mathbf{M}_t^i] = \int_0^{l'} [\mathbf{N}_w^i]^T \rho^i A^i(x^i)[\mathbf{N}_w^i]\,\mathrm{d}x^i, \quad (23)$$

TABLE 2

The fundamental frequency parameter λ_E of a uniform rotating cantilever Euler–Bernoulli beam with $\psi = 0°$

	λ_{E1}		λ_{E2}		λ_{E3}	
η/R	0·0	1·0	0·0	1·0	0·0	1·0
0·0	3·51602	3·51602	22·0348	22·0348	61·7049	61·7049
	3·5160†	3·5160†	22·0345†	22·0345†	61·697214‡	61·697214‡
2·0	4·13733	4·83371	22·6153	23·3664	62·2808	63·0751
	4·1373†	4·6337†	22·6149†	23·3660†	62·273184‡	63·067548‡
4·0	5·58503	7·47511	24·2737	26·9577	63·9742	66·9941
	5·5850†	7·4751†	24·2734†	26·9773†	63·966676‡	66·986772‡
6·0	7·36043	10·4440	26·8095	32·0280	66·6912	72·9939
	7·3604†	10·4439†	26·8091†	32·0272†	66·683914‡	72·986335‡
8·0	9·25694	13·5077	29·9959	37·9552	70·3002	80·5382
	9·2568†	13·5074†	29·9954†	37·9538†	70·292962‡	80·529532‡
10·0	11·2025	16·6070	33·6411	44·3707	74·5670	89·1673
	11·2023†	16·6064†	33·6404†	44·3682†	74·649295‡	89·156329‡

† Reference [9]; ‡ reference [8].

$$[\mathbf{M}_t^i] = \int_0^{l^i} [\mathbf{N}_\theta^i]^T \rho^i I_{yy}^i(x^i)[\mathbf{N}_\theta^i]\,\mathrm{d}x^i, \tag{24}$$

where $[\mathbf{M}_t^i]$, and $[\mathbf{M}_r^i]$ are the elemental mass matrix due to translational deformation, and the elemental rotary inertia mass matrix due to rotation, respectively. The explicit expressions of the entries of these respective elemental matrices are given in reference [16]. The composite elemental mass matrix of the ith beam element can also be obtained by summing up the contribution of each mass matrix, namely,

$$[\mathbf{M}^i] = [\mathbf{M}_t^i] + [\mathbf{M}_r^i], \tag{25}$$

where $[\mathbf{M}^i]$ is the elemental composite mass matrix, and is known as the consistent mass matrix because it is formulated using the same shape functions $[\mathbf{N}_w^i]$ and $[\mathbf{N}_\theta^i]$ that are used to formulate the stiffness matrix.

2.4. POTENTIAL ENERGY EXPRESSION

The potential energy V^i per unit volume of the beam element due to the centrifugal force F_z^i acting on the beam in the z-direction is given by

$$V^i = -\frac{1}{2}\int_0^{l^i} F_z^i w^i A^i(x^i)\,\mathrm{d}x^i \tag{26}$$

where

$$F_z^i = \rho^i(x^i)\Omega^2 w^i \sin^2\psi. \tag{27}$$

Equation (26) can be written in the matrix form as

$$V^i = -\tfrac{1}{2}\{\mathbf{q}^i\}^T(\Omega^2[\mathbf{M}_t^i]\sin^2\psi)\{\mathbf{q}^i\}. \tag{28}$$

TABLE 3

Effect of setting angle on the first four frequency parameters λ_T of uniform rotating cantilever Timoshenko beam with $R = 3$ and $\eta = 10$

	$(r_g/L)\rightarrow$	0·1		0·05	
	ψ	0°	90°	0°	90°
λ_{T1}	Present work	23·0060	20·8321	23·5220	21·2816
	Reference [14]	23·050	20·867	23·524	21·313
λ_{T2}	Present work	45·8150	45·0809	56·0951	55·2570
	Reference [14]	45·598	45·115	56·105	55·284
λ_{T3}	Present work	68·9308	67·3641	97·1537	96·7106
	Reference [14]	67·716	67·520	97·188	96·747
λ_{T4}	Present work	73·0185	72·7188	144·395	144·115
	Reference [14]	74·1677	72·756	144·490	144·208

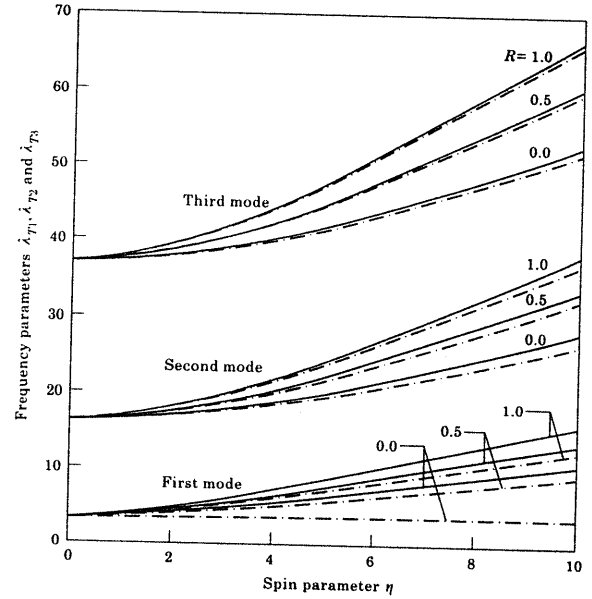

Figure 3. Variation of the first three frequency parameters of rotating uniform Timoshenko beam with $(r_g/L) = 0{\cdot}08$. ——, $\psi = 0°$; ------, $\psi = 90°$.

3. THE GENERALIZED EIGENVALUE PROBLEM

The sum of the individual element energies over the entire beam may be utilized to establish the Lagrangian function as

$$\mathscr{L} = \sum_{i=1}^{n} (T^i - U^i - V^i) \tag{29}$$

Upon substitution of the expression of $\mathscr{L}$ into Lagrange's equation of free vibrational motion

$$\frac{\mathrm{d}}{\mathrm{d}t}\left(\frac{\partial \mathscr{L}}{\partial \dot{q}^i}\right) - \frac{\partial \mathscr{L}}{\partial q^i} = 0, \tag{30}$$

one obtains the governing differential equation of motion of the rotating tapered beam. This may be written as

$$[\mathbf{M}]\{\ddot{\mathbf{q}}\} + ([\mathbf{K}_{e,s}] + \Omega^2([\mathbf{K}_c] - [\mathbf{M}_t]\sin^2\psi))\{\mathbf{q}\} = \{\mathbf{0}\}, \tag{31}$$

where $\{\mathbf{q}\}$ is the vector of all nodal co-ordinates of the beam. The matrices $[\mathbf{M}]$, and $[\mathbf{M}_t]$ are the global mass and, translational mass matrices while $[\mathbf{K}_{es}]$ and $[\mathbf{K}_c]$ represent global elastic stiffness matrix and centrifugal stiffness matrix, respectively, of the whole beam obtained by the standard finite element assembly procedure. It is clear from equation (31) that there are two competing effects produced by the rotation, a stiffening one, $\Omega^2[\mathbf{K}_c]$ and a softening one, $-\Omega^2[\mathbf{M}_t]\sin^2\psi$. The contribution of the gyroscopic term is assumed to be very small and hence is neglected in this paper. Assuming the solution of equation (31) in the form

$$\{\mathbf{q}\} = \{\bar{\mathbf{q}}\}\, e^{i\omega t}, \tag{32}$$

one obtains the generalized eigenvalue problem as

$$([\mathbf{K}_{es}] + \Omega^2([\mathbf{K}_c] - [\mathbf{M}_t]\sin^2\psi) - \omega^2[\mathbf{M}])\{\bar{\mathbf{q}}\} = \{\mathbf{0}\}, \tag{33}$$

where $\{\bar{\mathbf{q}}\}$ is a vector of displacement amplitudes and ω is the frequencies of harmonic vibrations. Solution of the generalized eigenvalue problem associated with equation (33) gives the natural frequencies and the corresponding mode shapes of the rotating tapered Timoshenko beam.

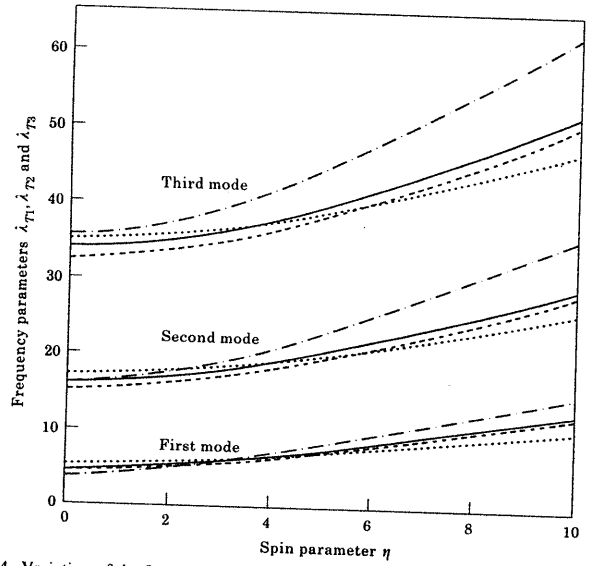

Figure 4. Variation of the first three frequency parameters of rotating tapered Timoshenko beam with $(r_g/L) = 0{\cdot}08$, $R = 1{\cdot}0$ and $\psi = 0°$. ——, $v_y = 0{\cdot}10$, $v_z = 0{\cdot}25$; – – – –, $v_y = 0{\cdot}30$, $v_z = 0{\cdot}60$; ——, $v_y = 0{\cdot}50$, $v_z = 0{\cdot}50$, ·····, $v_y = 0{\cdot}75$; $v_z = 0{\cdot}50$.

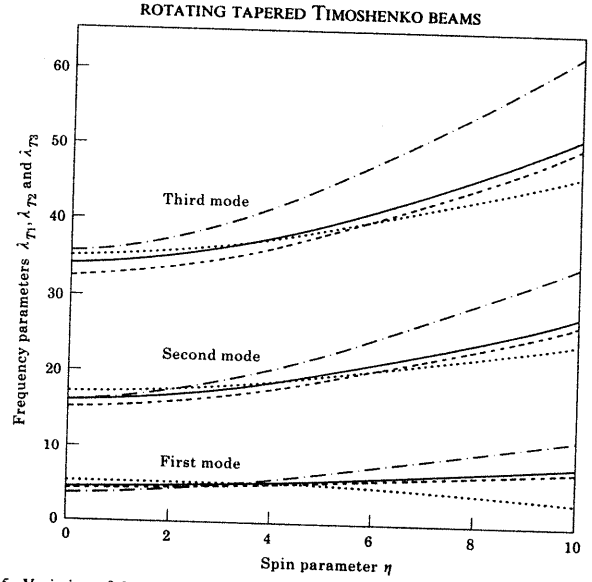

Figure 5. Variation of the first three frequency parameters of rotating tapered Timoshenko beam with $(r_g/L) = 0{\cdot}08$, $R = 1{\cdot}0$ and $\psi = 90°$. Key as for Figure 4.

4. RESULTS AND DISCUSSION

The case of a rotating tapered Timoshenko beam including the effects of hub radius and setting angle has been studied extensively. The results obtained in this investigation may be applied to tapered and uniform beams with doubly symmetric cross-sections. Because results for rotating tapered Timoshenko beams including the effects of hub radius and setting angle could not be found in the available literature, several special cases were examined to verify and validate the present scheme.

The case of a uniform Euler–Bernoulli beam has been reproduced here for various values of spin and hub radius parameters, as shown in Table 2. The present results were obtained by dividing the rotating beam into 10 finite beam elements of equal length and include the first three flexural frequency parameters for the flapping vibration ($\psi = 0°$). The results presented herein show very good agreement with other numerical techniques, namely, those presented by Hodges and Rutkowski [8] and Wright *et al.* [9].

Because the literature lacks sufficient information to adequately reproduce the same results based on Timoshenko theory, the following data are used: Poisson's ratio = 0·3, and shear correction factor = 0·85 for rectangular cross-section with $(r_g/L) = 0{\cdot}08$, this case being the most encountered in the literature. These results were obtained by using 10 finite Timoshenko beam elements. The numerical results

show that the effect of shear deformation and rotary inertia is more pronounced for beams at higher modes rather than at lower modes, as expected. The first four flapping ($\psi = 0°$) and lead-lag ($\psi = 90°$) natural frequencies of vibration of rotating uniform Timoshenko beams have been reproduced in Table 3. These results represent a very good agreement when compared to Yokoyama [14].

In order to study the effects of taper ratios, shear deformation, rotary inertia, hub radius, setting angle and spin parameter on the frequencies of a rotating tapered Timoshenko beam, a variety of results of simulations are presented in graphical form, as shown in Figures 3–5. A closer investigation to the fundamental mode is displayed by Figures 6–8.

In Figure 3, are shown the first three frequency parameters for both out-of-plane ($\psi = 0°$) and in-plane ($\psi = 90°$) vibration of a rotating uniform Timoshenko beam at different values of the hub radius parameter R and spin parameter η. These frequency parameters experience an increase with the increase of spin parameter and hub radius parameter. Furthermore, it is noteworthy to observe that as the spin parameter η increases, the difference between the out-of-plane and the in-plane vibration frequency parameters increase. This difference is highest for the fundamental mode and decreases as the mode number increases.

Figures 4 and 5 show respectively the first three frequency parameters for out-of-plane and in-plane vibration at different values of taper ratios and spin rate

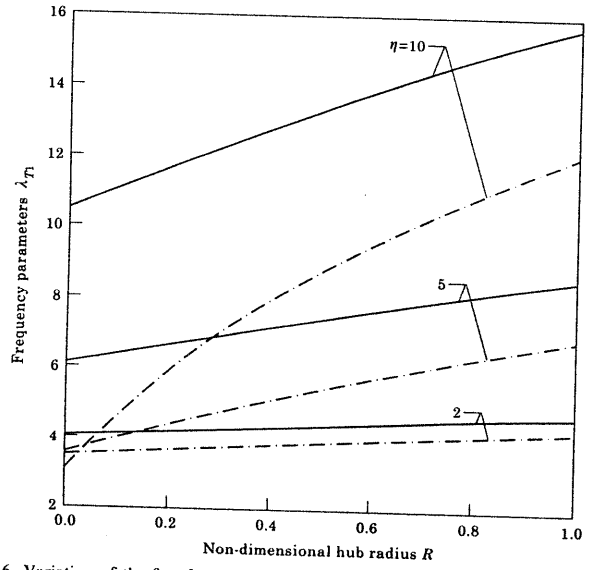

Figure 6. Variation of the first frequency parameter λ_{Ti} of rotating tapered Timoshenko beam Variation of the first frequency with $(r_x/L) = 0{\cdot}08$, $\nu_y = \nu_z = 0{\cdot}1$. ——, $\psi = 0$; and - - - -, $\psi = 90°$.

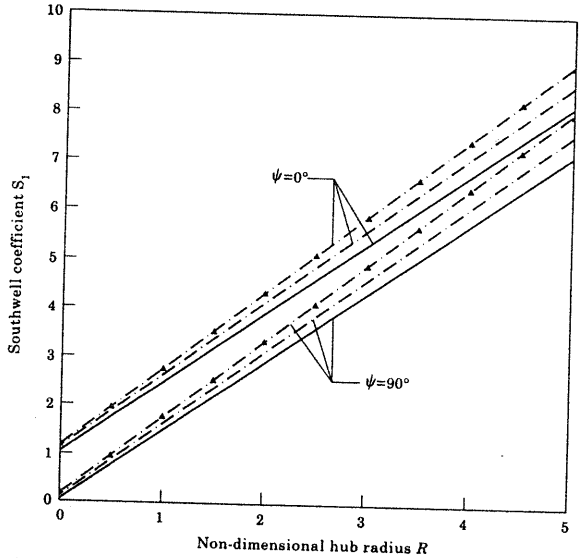

Figure 7. Southwell coefficient S_1 as a function of hub radius R of a uniform beam for two extreme setting angles. Present solution : —, Euler: $S_1 = 1{\cdot}1456 + 1{\cdot}4855\ R - \sin^2\psi$; ——, Timoshenko: $S_1 = 1{\cdot}0484 + 1{\cdot}4170\ R - \sin^2\psi$. Shilhansl: —▲—, Euler: $S_1 = 1{\cdot}173 + 1{\cdot}5584\ R - \sin^2\psi$.

while keeping a constant value of the hub radius parameter ($R = 1$). From these figures it can also be noticed that for tapered Timoshenko beams, all the three frequency parameters experience an increase as the spin parameter increases. In addition to that, a cross-over between the frequencies of the beam at different tapers can be noticed. Moreover, it is interesting to observe the dominance of the softening effect over the stiffening one which is manifested by Figure 5 and characterized by a decrease in the fundamental frequency parameter at high spin parameters for the case of $\nu_y = 0{\cdot}75$ and $\nu_z = 0{\cdot}5$. Such a decrease shows that the term $-\Omega^2[\mathbf{M}_t]\sin^2\psi$ dominates the centrifugal effect, thus resulting in a net softening effect at $\psi = 90°$ and higher values of η. Furthermore, the previous figures show that the out-of-plane frequency parameters are always greater than those of the corresponding in-plane frequency; this was shown to be the case for a uniform Euler–Bernoulli beam (see reference [22] for proof) and the present results suggest that this conclusion can be extended to the uniform and tapered Timoshenko beam.

The fundamental frequency parameter of flexural vibration is examined at a wide range of spin parameter and hub radius parameter for two extreme setting angles $\psi = 0°$ and $\psi = 90°$ as shown in Figure 6. For higher spin parameters, the frequency dependence on R depends strongly on the setting angle ψ; thus for

$\psi = 0°$, the fundamental frequency is still near linear with hub radius parameter R, but for $\psi = 90°$, not only is the relationship no longer linear, but also shows much greater sensitivity to changes in hub radius; this is due to the relative contributions of both stiffening and softening effect, the former depending on R, the latter on ψ. On the other hand, it is of interest to notice again the dominance of the softening effect over the stiffening effect for the case of $R = 0$ and $\eta = 10$. Moreover, one can also observe that for a fixed η, the difference between the flapping and lead-lag frequency decreases as the hub radius increases. The larger the spin is, the greater the difference among the frequencies is manifested as shown in Figure 6.

It is of interest to investigate whether the flexural frequencies of rotating cantilever tapered Timoshenko beams would fit into some form of Southwell linear approximation. The flexural frequency parameter λ_i of a rotating beam is usually expressed as a function of the corresponding frequency parameter at standstill λ_0, and the spin parameter η_i, in the form $\lambda_i^2 = \lambda_0^2 + S_i\eta_i^2$, where the subscript i refers to the ith mode and S_i is called Southwell coefficient. It is worthwhile trying to fit the results of simulation into Southwell form and obtain Southwell coefficients for several parameter changes. Results presented in this form are more economical

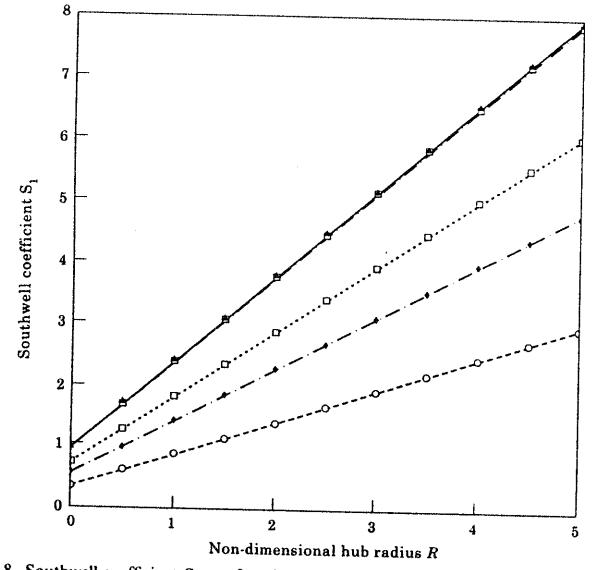

Figure 8. Southwell coefficient S_1 as a function of hub radius R for a tapered Timoshenko beam, $(r_g/L) = 0{\cdot}08$ and $\psi = 0°$. ---□---, $v_y = 0{\cdot}1$, $v_z = 0{\cdot}0$, $S_1 = 1{\cdot}01468 + 1{\cdot}37639\ R$; —▲—, $v_y = 0{\cdot}0$, $v_z = 0{\cdot}1$, $S_1 = 1{\cdot}01761 + 1{\cdot}38132\ R$; ····□····, $v_y = 0{\cdot}4$, $v_z = 0{\cdot}3$, $S_1 = 0{\cdot}75948 + 1{\cdot}06279\ R$; —◆—, $v_y = 0{\cdot}5$; $v_z = 0{\cdot}5$, $S_1 = 0{\cdot}59444 + 0{\cdot}84169\ R$; --○---, $v_y = 0{\cdot}6$; $v_z = 0{\cdot}8$, $S_1 = 0{\cdot}37693 + 0{\cdot}52446\ R$.

and useful from practical point view than a long table of frequency parameters at various values of parameter changes. Schilhansl [2] presented an explicit expression of S_1 corresponding to the fundamental mode of a rotating uniform Euler–Bernoulli beam. Dokainish and Rawtani [21] presented a table of values of S_i up to third mode of vibration of rotating cantilever plates.

In this analysis an attempt has been made for the first time to obtain Southwell coefficients for the fundamental mode of rotating uniform and tapered Timoshenko beams. Figure 7 shows the Southwell coefficient S_1 as a function of hub radius parameter R and setting angle ψ. Explicit expressions of S_1 for rotating uniform Euler–Bernoulli and Timoshenko beams are also presented in this figure. It is of interest to observe that S_1 corresponding to the flapping motion ($\psi = 0°$) is parallel to the one of lead-lag motion ($\psi = 90°$) and the difference between them is unity. A similar trend can be observed for the case of the Timoshenko beam. The expression S_1 corresponding to the rotating uniform Euler–Bernoulli beam is in excellent agreement when compared to the one proposed by Schilhansl [2].

Figure 8 displays the Southwell coefficient S_1 for rotating tapered Timoshenko beams. The corresponding explicit expressions of S_1 of the flapping motion of rotating tapered Timoshenko beams have been provided at a wide range of taper ratios. Lead-lag expressions of S_1 of rotating tapered Timoshenko beams can be obtained from the flapping case by considering the results obtained from Figure 7 and explained in the previous paragraph.

5. CONCLUSION

The modal characteristics of the free vibration of a tapered Timoshenko beam mounted on the periphery of a rotating rigid hub, at a setting angle with the plane of rotation, have been investigated. The finite element method is used to discretize the beam element. This formulation permits unequal breadth and depth taper ratios as well as unequal element lengths. The effects of shear deformation, rotary inertia, hub radius, setting angle, and spinning rotation are accounted for. It has been noticed that the softening effect $-\Omega^2[\mathbf{M}_t]\sin^2\psi$ can dominate the stiffening effect $\Omega^2[\mathbf{K}_c]$ under the conditions where ($\psi = 90°$ and $R = 0$) for high spinning rotation. Southwell coefficients have been reported for the first time up to the best knowledge of the authors for tapered Timoshenko beams. The results obtained stand in excellent agreement with the Southwell approximation. It is also shown that Southwell coefficients depend on setting angle ψ, hub radius parameter R and taper ratios v_y and v_z.

ACKNOWLEDGMENT

The support of King Fahd University of Petroleum and Minerals is greatly appreciated.

REFERENCES

1. R. L. SUTHERLAND 1949 *Journal of Applied Mechanics* **16**, 389–394. Bending vibation of a rotating blade vibrating in the plane of rotation.

2. M. SCHILHANSL 1958 *ASME Journal of Applied Mechanics* **25**, 28–30. Bending frequency of a rotating cantilever beam.
3. W. CARNEGIE 1959 *Journal Mechanical Engineering Science* **1**, 235–240. Vibrations of rotating cantilever blading: theoretical approaches to the frequency problem based on energy methods.
4. D. PNUELI 1972 *ASME Journal of Applied Mechanics* **39**, 602–604. Natural bending frequency comparable to rotational frequency in rotating cantilever beam.
5. L. H. JONES 1975 *Quarterly of Applied Mathematics* **33**, 193–203. The transverse vibration of a rotating beam with tip mass: the method of integral equations.
6. Y. A. KHULIEF and LAJEOON YI 1988 *Computers and Structures* **42**, 781–795. Lead-lag frequencies of a rotating beam with end mass.
7. S. V. HOA 1979 *Journal of Sound and Vibration* **67**, 369–381. Vibration of rotating beams with end mass.
8. D. H. HODGES and M. J. RUTKOWSKI 1981 *American Institute of Aeronautics and Astronautics Journal* **19**, 1459–1466. Free vibration analysis of rotating beams by a variable-order finite-element method.
9. A. D. WRIGHT, C. E. SMITH, R. W. THRESHER and J. L. C. WANG 1982 *ASME Journal of Applied Mechanics* **49**, 197–202. Vibration modes of centrifugally stiffened beams.
10. D. STORTI and Y. ABOELNAGA 1987 *ASME Journal of Applied Mechanics* **54**, 311–314. Bending vibration of a class of rotating beams with hypergeometric solutions.
11. Y. A. KHULIEF 1989 *Journal of Sound and Vibration* **134**, 87–97. Vibration frequencies of a rotating tapered beam with end mass.
12. R. O. STAFFORD and V. GIURGIUTIU 1975 *International Journal of Mechanical Sciences* **17**, 719–727. Semi-analytic method for rotating Timoshenko beams.
13. S. PUTTER and H. MANOR 1978 *Journal of Sound and Vibration* **56**, 175–185. Natural frequencies of radial rotating beams.
14. T. YOKOYAMA 1988 *International Journal of Mechanical Science* **30**. 743–755. Free vibration characteristics of rotating Timoshenko beams.
15. H. DU, M. K. LIM and K. M. LIEW 1994 *Journal of Sound and Vibration* **175**, 505–523. A power series solution for vibrations of a rotating Timoshenko beam.
16. A. BAZOUNE and Y. A. KHULIEF 1992 *Journal of Sound and Vibration* **156**, 141–164. A finite beam element for vibration analysis of rotating tapered Timoshenko beams.
17. Y. A. KHULIEF and A. BAZOUNE 1992 *Computers and Structures* **42**, 781–795. Frequencies of rotating tapered Timoshenko beams with different boundary conditions.
18. S. MULMULE, G. SINGH and G. VENKATESWARA RAO 1993 *Journal of Sound and Vibration* **160**, 372–377. Flexural vibrations of rotating tapered Timoshenko beams.
19. S. NAGULESWARAN 1994 *Journal of Sound and Vibration* **174**, 559–560. Comments on: Flexural vibrations of rotating tapered Timoshenko beams.
20. S. H. HSIEH and J. F. ABEL 1995 *Journal of Sound and Vibration* **182**, 91–107. Comparison of two finite element approaches for analysis of rotating bladed-disk assemblies.
21. M. A. DOKAINISH and S. RAWTANI 1971 *International Journal for Numerical Methods in Engineering* **3**, 233–248. Vibrations of rotating cantilever plates.
22. S. NAGULESWARAN 1994 *Journal of Sound and Vibration* **176**, 613–624. Lateral vibration of a centrifugally tensioned Euler–Bernoulli beam.

APPENDIX: NOMENCLATURE

$A^i(x^i)$	cross-sectional area of the beam element
A_0	cross-sectional area of the root of the beam
$[\mathbf{B}^i]$	strain displacement matrix
E	modulus of Elasticity

$\overline{F_x^i}(x^i)$	x-component of the centrifugal force
F_z^i	z-component of the centrifugal force
G	modulus of rigidity
$I^i(x^i)$	second moment of area of the beam
I_0	second moment of area at the root of the beam
i	refers to the ith element
$[\mathbf{K}^i]$	composite elemental stiffness matrix
$[\mathbf{K}_b^i]$	elemental bending stiffness matrix
$[\mathbf{K}_s^i]$	elemental shear stiffness matrix
$[\mathbf{K}_{cs}^i]$	$= [\mathbf{K}_b^i] + [\mathbf{K}_s^i]$ elemental stiffness matrix (due to bending and shear deformations)
$[\overline{\mathbf{K}_c^i}]$	elemental centrifugal stiffness matrix
$[\mathbf{K}_{cs}]$	$= [\mathbf{K}_c] + [\mathbf{K}_s]$ global stiffness matrix of the beam
κ	shear correction factor
$\mathscr{L}$	Lagrangian
L	truncated length of the beam
L^i	outboard length of the beam from element under consideration
L_{0y}	untruncated length of the beam in the (xy) plane
L_{0z}	untruncated length of the beam in the (xz) plane
l^i	element length
$[\mathbf{M}^i]$	composite elemental mass matrix
$[\mathbf{M}_t^i]$	elemental translational mass matrix
$[\mathbf{M}_r^i]$	elemental rotary inertia mass matrix
$[\mathbf{M}_t]$	translational mass matrix of the beam
$[\mathbf{M}]$	global mass matrix of the beam
$[\mathbf{N}_w^i]$, $[\mathbf{N}_\theta^i]$	matrices of shape funcitons
n	total number of elements
p^i	location of the finite element (i)
$\{\mathbf{q}\}$	vector of nodal co-ordinates
$\{\bar{\mathbf{q}}\}$	vector of displacement amplitudes of vibration
R_0	hub radius
R	$= R_0/L$, non-dimensional hub radius
r_g	$= \sqrt{I_0/A_0}$, radius of gyration of the cross-section of the beam
S_i	Southwell coefficients corresponding to ith mode.
t	time
T^i	kinetic energy of the beam element
U^i	strain energy of the beam element
V^i	potential energy of the beam element
w	total deflection in (xz) plane
w_b	deflection due to bending deformation
w_s	deflection due to shear deformation
x^i	elemental co-ordinate
xyz	local co-ordinate axes
XYZ	global co-ordinate axes
ρ^i	mass density
β_i	constants
μ_i	constants
ω	natural frequency of the beam
Ω	rate of spin of the hub
ψ	setting angle
Φ	shear deformation parameter
γ^i	angle of distorsion due to shear deformation
θ^i	angle of rotation due to bending deformation
λ	$= \omega L^2\sqrt{\rho A_0/EI_0}$, frequency parameter

λ_E Euler–Bernoulli frequency parameter
λ_T Timoshenko frequency parameter
η $= \Omega L^2/\sqrt{EI_0/\rho A_0}$, spin parameter
ξ^i $= x^i/l^i$, non-dimensional elemental co-ordinates
ν_y $= L/L_{0_y}$, taper ratio in (xy) plane
η_z $= L/L_{0_z}$, taper ratio in (xz) plane
$[\,]^T$ transpose of $[\,]$

Journal of Sound and Vibration (1999) **219**(1), 175–188
Article No. jsvi.1998.1852, available online at http://www.idealibrary.com.on IDEAL

LETTERS TO THE EDITOR

VIBRATION CONTROL OF A ROTOR SYSTEM BY DISK TYPE ELECTRORHEOLOGICAL DAMPER

G. Z. YAO AND Y. QIU
State Key Laboratory of Mechanical Structural Strength and Vibration, Xi'an Jiao Tong University, Xi'an 710049, *Shananxi, P.R.C.*

AND

G. MENG* AND T. FANG
Institute of Vibration Engineering, Northwestern Polytechnical University, Xi'an 710072, *Shaanxi, P.R.C.*

AND

Y. B. FAN
Foshan University, Foshan 528000, *Guangdong, P.R.C.*

(*Received* 3 *September* 1997, *and in final form* 22 *June* 1998)

1. INTRODUCTION

Electrorheological (ER) fluid is a kind of smart material which has the merits of fast response, easy control and low energy consumption. It has a broad application to vibration control. Since Winslow [1] first reported the ER effect in 1947, many achievements have been obtained in vibration control [2–5]. The application of ER fluid to the vibration control of rotor systems was first proposed by Nikolajsen and HOQUE [3]. Through experiments they demonstrated the capability of the application of ER fluid in rotor systems. The resonant vibration around the first critical speed was suppressed by the ER damper. In this paper, a new disk type ER damper is designed and its application to the vibration suppression of a rotor system is investigated theoretically and experimentally. Both the suppression of the resonant vibration around the first critical speed and the suppression of the large response caused by the sudden unbalance are considered.

2. STRUCTURE OF ER DAMPER AND EXPERIMENTAL ARRANGEMENT

The new designed ER damper consists of a moving part with 4 disks and a stationary part with 5 disks. The disks are placed uniformly and alternatively with a uniform gap of 1·7 mm. For clarity, only a part of them is shown in Figure 1. The stationary part is connected to the negative pole of the electric field, while the moving part to the positive one.

The experimental rig is composed of a shaft, a disk D, an ER damper, and a motor, as shown in Figure 2. The shaft is 9·5 mm in diameter and 500 mm in length. The moving part of the ER damper, together with the outer ring of the bearing B, is mounted on a squirrel cage. Both of them move in the same way. The shaft is driven by a d.c. motor, the speed of which may be adjusted continually from 0 to 12 000 rpm.

*Now at Foshan University, Foshan 528000, Guangdon, P.R.C.

0022-460X/99/010175 + 14 $30.00/0